Original Article

Changes in the renal artery and renal volume and predictors of renal atrophy in patients with complicated type B aortic dissection after thoracic endovascular aortic repair

Yi-Tong Yu[1], Xin-Shuang Ren[1], Yun-Qiang An[1], Wei-Hua Yin[1], Jie Zhang[1], Xiang Wang[2], Bin Lu[1]

[1]Department of Radiology, Fuwai Hospital, Peking Union Medical College & Chinese Academy of Medical Sciences, Beijing, China; [2]Department of Cardiology, Beijing Hospital, Peking Union Medical College & Chinese Academy of Medical Science, Beijing, China

Contributions: (I) Conception and design: YT Yu, B Lu, XS Ren, WH Yin; (II) Administrative support: B Lu; (III) Provision of study materials or patients: YT Yu, X Wang; (IV) Collection and assembly of data: YT Yu, X Wang, J Zhang; (V) Data analysis and interpretation: YT Yu, YQ An; (VI) Manuscript writing: All authors; (VII) Final approval of manuscript: All authors.

Correspondence to: Bin Lu, MD. Department of Radiology, Fuwai Hospital, Peking Union Medical College & Chinese Academy of Medical Sciences, Beijing, China; State Key Lab and National Center for Cardiovascular Diseases, Beijing, China. Email: blu@vip.sina.com.

Background: For complicated Stanford type B aortic dissection (TBAD), thoracic endovascular aortic repair (TEVAR) is the recommended treatment; however, the type of renal artery that should be repaired remains controversial. The study aimed to investigate the changes in the renal artery and renal volume in complicated TBAD after TEVAR and the predictors of renal atrophy.

Methods: The cohort study retrospectively enrolled patients with acute and subacute complicated TBAD who underwent aortic computed tomography angiography (CTA) 1 month before as well as 1 week and half a year after TEVAR from January 2010 to May 2017. According to the source of blood supply shown in preoperative CT, the renal artery was classified in 3 ways: type 1, supplied by the aortic true lumen; type 2, supplied by the aortic false lumen; or type 3, supplied by both the true and false lumen.

Results: A total of 91 patients (81 men and 10 women) with an average age of 48.12±10.35 years were enrolled. Renal arteries were classified as type 1 (n=91), type 2 (n=35), and type 3 (n=56). There was no difference in the distribution of the 3 types on the left and right sides (type 1 *vs.* type 2 *vs.* type 3: 52:39 *vs.* 15:20 *vs.* 24:32; P=0.152). After TEVAR, type 3 was more likely to have spontaneous healing than type 2 (16.1% *vs.* 2.9%; P=0.049). There was no significant difference in the preoperative volume of kidneys of the 3 types (type 1 *vs.* type 2 *vs.* type 3: 198.23±38.68 *vs.* 197.37±41.77 *vs.* 195.10±36.11 mL; P=0.893). The postoperative volume of types 2 and 3 was smaller than that of type 1 (type 1 *vs.* type 2 *vs.* type 3: 190.09±43.25 *vs.* 165.15±52.63 *vs.* 170.70±45.28 mL; P=0.006). The renal volume was reduced in all 3 types of renal artery, especially in type 2 (the change of renal volume for type 1 *vs.* type 2 *vs.* type 3: –8.14±29.31 *vs.* –32.22±41.59 *vs.* –24.41±38.44 mL; P=0.001). The relative change of renal volume for type 1 *vs.* type 2 *vs.* type 3: (–3.64±15.69)% *vs.* (–16.00±21.29)% *vs.* (–11.97±18.22)%; P=0.001). During the median follow-up of 668 days, 7 patients (7.7%) belonging to types 2 and 3 developed renal atrophy. False lumen thrombosis in the abdominal aorta and/or the renal artery was the predictor of renal atrophy [hazard ratio (HR) =17.757; P=0.008].

Conclusions: Patients with type 2 or 3 renal artery and false lumen thrombosis in the abdominal aorta and/or renal artery should be monitored closely and actively intervened to prevent renal atrophy.

Keywords: Type B aortic dissection (TBAD); renal artery; renal volume; renal atrophy; thoracic endovascular aortic repair (TEVAR)

Submitted Dec 29, 2021. Accepted for publication Jul 22, 2022.
doi: 10.21037/qims-21-1240
View this article at: https://dx.doi.org/10.21037/qims-21-1240

Introduction

The renal artery is one of the most common branches involved in aortic dissection (1). Unlike other abdominal branches, the renal artery is a telangion without potential cross-perfusion through rich collateral flow. Renal artery dissection could result in renal malperfusion, which reportedly reduces kidney function and causes kidney shrinkage (2,3) and could even be the most important risk factor for increased mortality (4-6). With recent advances in endovascular stenting, thoracic endovascular aortic repair (TEVAR) is recommended for Stanford type B aortic dissection (TBAD) (7). However, the criteria for renal artery stenting remains controversial. Conventionally, renal function is revealed by the glomerular filtration rate; however, the rate remains normal in severe unilateral renal atrophy (8). Unilateral renal function can be evaluated by renal perfusion and blood flow in the renal arteries measured by ultrasound, magnetic resonance imaging, and digital color-coded digital subtraction angiography (DSA) (9). However, these methods have limitations that make them difficult to use in clinical practice. It is reported that renal volume is a surrogate marker of renal artery perfusion (3). Renal volume correlates well with single kidney glomerular filtration rate in native kidneys (10,11) and is an excellent predictor of single renal function (1,12). Monitoring renal atrophy through computed tomography (CT) might provide early evidence of renal injury (8). It is particularly important to focus on the change in renal volume and renal atrophy in patients with TBAD who often have hypertension or atherosclerosis that puts them at additional risk of renal injury (8,13). Even unilateral renal atrophy deserves our attention in preventing the rapid deterioration of renal function due to urinary tract infection, urinary tract obstruction, and the use of kidney-damaging drugs.

This retrospective observational study aimed to investigate the natural history of the involved renal artery and the change in the renal volume in patients with TBAD after TEVAR and to identify the predictors associated with renal atrophy. We present the following article in accordance with the STROBE reporting checklist (available at https://qims.amegroups.com/article/view/10.21037/qims-21-1240/rc).

Methods

Patients

Stanford classifies dissections into 2 types based on whether the ascending aorta is involved. When the ascending aorta is not involved, it is classified as type B (14). Patients diagnosed with TBAD by aortic CT angiography (CTA) were searched by picture archiving and communication systems (PACS), and the time of CT examinations was obtained. Baseline characteristics and clinical course were obtained from the medical records. The retrospective cohort analyzed patients diagnosed with acute (<14 days) and subacute (15–90 days) complicated TBAD from January 2010 to May 2017 in Fuwai Hospital. The inclusion criteria were the following: (I) patients who underwent preoperative aortic CTA and had TEVAR within 1 month; (II) patients who had an aortic CTA examination 1 week and half a year after TEVAR; (III) patients with different renal artery involvement types in the preoperative CTA (discussed in section *Definition of the type of renal artery involvement*); (IV) patients who did not have initial renal atrophy due to end-stage renal disease or previous renal insult; (V) patients who had no history of nephrectomy; (VI) patients who did not have >50% stenosis in the preoperative renal artery. The exclusion criteria were the following: (I) stenting in the renal artery in the follow-up CT and (II) patients who lacked clinical data (n=18). The remaining 91 patients were enrolled in this study. The study was conducted in accordance with the Declaration of Helsinki (as revised in 2013). The study was approved by the Ethics Committees of Fuwai Hospital, and informed consent was taken from all individual participants.

CT scan

CT examination was performed with various scanners, including Revolution CT (GE Healthcare, Waukesha, WI, USA), Brilliance Ict (Philips Healthcare, Cleveland, OH, USA), and SOMATOM Definition Flash (Siemens Healthcare, Forchheim, Germany). The scan range was set from the level of the thoracic inlet to the pubic symphysis. All scans were reconstructed with 0.625, 0.75, 1, or 1.5 mm slices. A tube potential of 120, 100, and 80 kV was used for patients with a body mass index (BMI) >30, 20–30, and <20 kg/m^2, respectively. The X-ray tube current was adjusted automatically. The contrast-enhanced acquisition was performed with an intravenous bolus injection of iodinated contrast medium (iopromide 370 mgI/mL; Ultravist, Bayer Healthcare, Leverkusen, Germany) at a volume of 1 mL/kg body weight with a saline chaser of 40 mL at a rate of 4–5 mL/s. Automated bolus tracking was applied with a circular region of interest positioned at the level of the

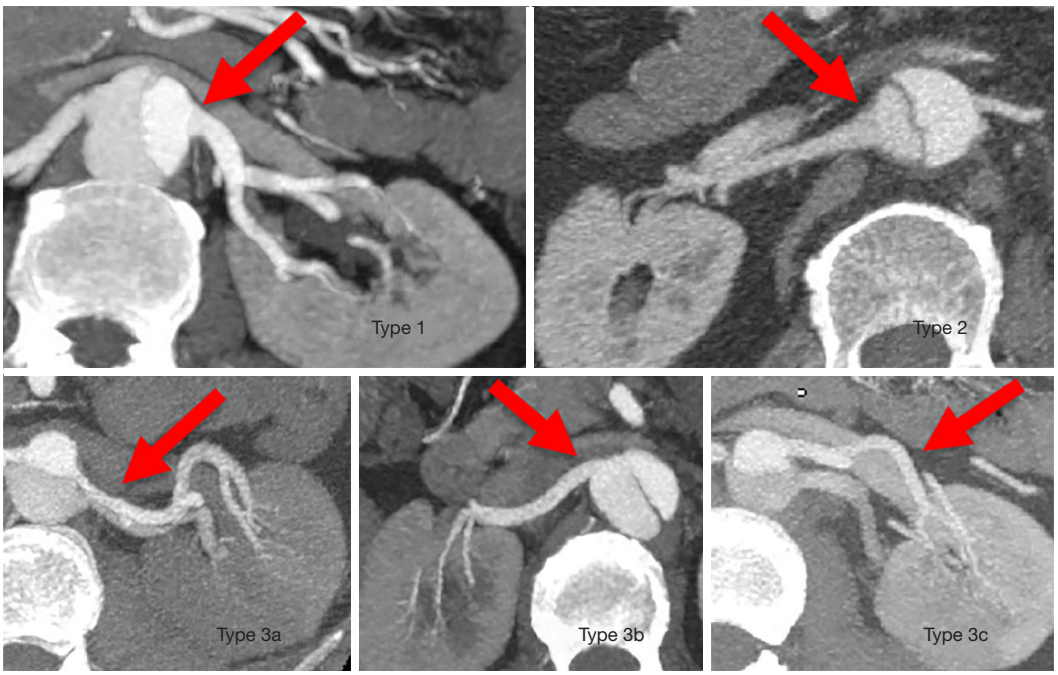

Figure 1 Illustrative examples of different types of renal artery involvement. Type 1: renal arteries supplied by the aortic true lumen (red arrow) exclusively. Type 2: renal arteries supplied by the aortic false lumen (red arrow) exclusively. Type 3: renal arteries supplied by both the aortic true and false lumen (red arrow), with (type 3a) or without (type 3b) the flap extended into the branches and with double renal arteries where one is from the true lumen and the other is from the false lumen (type 3c).

descending aorta. Data acquisition was started 6 seconds after the CT value reached a threshold of 100 HU. The raw data of the scans were transferred to the workstation (Advantage Workstation Release 4.6 software, GE Healthcare) for 3-dimensional image reconstruction and measurement.

Definition of the type of renal artery involvement

According to the source of blood supply, the types of renal artery involvement were delineated as follows: type 1, renal arteries supplied by the aortic true lumen exclusively; type 2, renal arteries supplied by the aortic false lumen exclusively; and type 3, renal arteries supplied by both the aortic true and false lumen, including renal arteries with or without an extended flap and accessory renal arteries or double renal arteries with one originating from the true lumen and the other from the false lumen (7). Illustrative examples of each type are detailed in *Figure 1*. Although all 3 types involved renal arteries, type 2 and type 3 were defined as the affected arteries. During the evaluation of the change in renal artery morphology, the phenomenon of the renal artery pattern changing to type 1 from another type without renal artery stent placement was defined as spontaneous healing (1).

Image analysis

Renal artery involvement was classified according to preoperative CT images. The preoperative and the last follow-up CT images were evaluated for the change in the type of renal artery and renal volume. The CT 1 week after TEVAR was used to assess the CT signs, which could predict renal atrophy.

False lumen thrombosis in CTA refers to a filling defect in the false lumen of the aorta and/or the renal artery. Renal volume was defined as the combined volume of the renal medulla and renal cortex, without any renal cyst or the renal pelvis (1). Each kidney was labeled on the postprocessing workstation, and its volume was automatically measured. The change in renal volume as well as the difference between the follow-up renal volume (V') and the preoperative renal volume (V) for each type was investigated. To evaluate the impact of preoperative kidney condition, the relative change of renal volume,

which was described as the change of renal volume relative to the preoperative volume [(V'–V)/V×100%], was also assessed. Follow-up on the renal relative volume change of the bilateral kidney, $(V'_1–V'_{2or3})/V'_1$, where one kidney was supplied by type 1 (V'_1) and the other was supplied by type 2 or 3 (V'_{2or3}), was performed. To avoid bilateral renal volume reduction after TEVAR due to aging or systemic disease, renal atrophy was defined as follows: $(V'_1–V'_{2or3})/V'_1$ >50% (8,14). The numbers of patients with renal malperfusion and spontaneous healing after TEVAR were analyzed. Renal malperfusion was defined as the CT evidence of ischemia, specifically, a wedge-shaped area of decreased density in renal parenchyma consistent with vascular distribution or overall renal density decreased on both sides or one side. The true and false lumen size was the maximum vertical distance between the lumen wall and the tangent of the intimal flap at the level of the affected renal artery. The relative size of the false lumen was the ratio of the size of the false lumen to that of the true lumen. The relative enhancement of the affected renal artery was the ratio of CT values of the affected renal artery to that of the true lumen at the same level.

A radiologist with more than 5 years of experience in cardiovascular imaging who was blinded to the clinical status and unaware of follow-up results evaluated the CTA images. When in doubt, another radiologist with 10 years of experience would participate and reach a final consensus reading according to the definitions described above.

Statistical analysis

Continuous variables, including relative change in renal volume, were tested for normal distribution with the Kolmogorov-Smirnov test. Continuous variables with a normal distribution are expressed as mean ± standard deviation and were compared using the independent samples *t*-test. Meanwhile, variables without a normal distribution are expressed as median and interquartile range and were compared using the Mann-Whitney U test. According to the variables concerning the characteristics of renal artery and kidney among the 3 types of renal artery involvement, analysis of variance (ANOVA) was performed to compare the continuous variables. Categorical variables are described as number and percentage and were compared with the Pearson chi-squared test, Fisher exact test, and continuity correction test as appropriate. The paired *t*-test was used to compare serum creatinine, estimated glomerular filtration rate (eGFR), and urea nitrogen before and after TEVAR. The Cox proportional hazards model was applied to identify those factors associated with renal atrophy. The Kaplan-Meier method was applied for survival analysis, and the log-rank test was performed. Statistical analysis was performed with SPSS version 18.0 (IBM Corp., Armonk, NY, USA). All P values were 2-sided, with a P value <0.05 being considered statistically significant. A box plot was generated with GraphPad Prism 8 software (GraphPad Software, Inc., San Diego, CA, USA). The Kaplan-Meier curve was performed using MedCalc for Windows (version 15.2.2, MedCalc Software, Ostend, Belgium).

Results

Patient demographics

A total of 91 patients (81 men and 10 women) with an average age of 48.12±10.35 years were included. The baseline characteristics of enrolled patients are described in *Table 1*. A total of 182 branches with preoperative and postoperative CTA were analyzed. The median interval between preoperative CT and postoperative CT was 668 days (Q25: 356.5, Q75: 1,231.5). Antihypertensives were prescribed to 84 (92.31%) patients at discharge. During follow-up, 7 patients (7.69%) suffered from renal atrophy (3 were type 2; 4 were type 3), serum creatinine increased in 2 patients (2.20%), and urea nitrogen increased in 22 patients (24.2%). There were no significant differences in serum creatinine, eGFR, or urea nitrogen before and after TEVAR (serum creatinine: 97.98±27.00 *vs.* 96.11±27.88, P=0.690; eGFR: 151.55±63.07 *vs.* 144.38±60.91, P=0.471; urea nitrogen: 6.10±1.98 *vs.* 6.59±1.91; P=0.068).

Characteristics and changes of renal arteries and kidneys

Renal artery involvement was categorized based on preoperative CTA as type 1 (n=91), type 2 (n=36), and type 3 (n=55). In the type 3 group, 3 patients had static stenosis of the renal artery with false lumen thrombosis along the vessel. All of the other patients had dynamic stenosis. Although there was no significant difference in the left and right distribution of the 3 types (type 1, 52:39; type 2, 15:20; type 3, 24:32; P=0.152), type 1 was more often distributed in the left, while type 2 and 3 were more often distributed in the right. Spontaneous healing was more likely to occur in type 3 than type 2 (16.1% *vs.* 2.9%; P=0.049). Follow-up showed that the 3 types could transition into each other. For example, 1 renal artery changed from type 1 to type 3, 4 renal arteries changed from type 2 to type 3, and 3 renal

Table 1 Baseline characteristics of enrolled patients

Parameters	Total (n=91)
Age (years)*	48.12±10.35
Male, n (%)	81 (89.01)
BMI (kg/m^2)*	26.63±4.43
Symptom, n (%)	
Chest pain	72 (79.12)
Back pain	45 (49.45)
Abdominal pain	10 (10.99)
Hypertension, n (%)	68 (74.73)
Elevated blood pressure on admission, n (%)	19 (20.88)
Diabetes, n (%)	5 (5.49)
History of smoking, n (%)	40 (43.96)
Elevated preoperative serum creatinine (>133 μmol/L), n (%)	5 (5.49)
Elevated preoperative blood urea nitrogen (>7.9 μmol/L), n (%)	14 (15.38)
eGFR (mL/min per 1.73 m^2)*	136.02±58.95
False lumen thrombosis in preoperative CTA, n (%)	37 (40.66)
In thoracic aorta	31 (34.07)
In abdominal aorta	12 (13.19)
In renal artery	3 (3.30)
Antihypertensive prescribed to the patient at discharge	84 (92.31)
Interval between preoperative and postoperative CTA (days)#	668 (356.5, 1,231.5)

*, data are the means ± standard deviation; #, data are the median (Q25, Q75). BMI, body mass index; eGFR, estimated glomerular filtration rate; CTA, computed tomography angiography.

arteries changed from type 3 to type 2. Before TEVAR, renal malperfusion was more common in kidneys supplied by type 2 (42.86%) and type 3 (46.43%) than in type 1 (3.30%), with statistical differences (P<0.001). However, no significant difference was found in renal volume among the 3 types (P=0.893). In the follow-up, renal malperfusion was more frequently found in type 2 (54.29%), followed by type 3 (23.21%) and type 1 (2.20%), with statistical differences (P<0.001). The follow-up volume of kidneys supplied by the 3 types all decreased, especially type 2 and type 3 (P=0.006). The reduction in volume in type 2 and type 3 was significantly more than that in type 1 (P=0.001). The renal artery and kidney characteristics of different involvement types are detailed in *Figure 2* and *Table 2*.

With consideration to the preoperative renal volume, the relative renal volume change of type 1 was significantly smaller than that of the others (P=0.001). *Figure 3* shows the percentage relative change of the renal volume in the 3 groups based on the types of renal artery involvement. Relative renal volume change of type 1 (–3.64±15.69)% was significantly smaller compared with type 2 [(–16.00±21.29)%; *t*-test, P<0.001] and type 3 [(–11.97±18.22)%; *t*-test, P=0.006]. No significant difference in relative change of renal volume was found between type 2 and type 3 (P=0.289).

CT findings predicting renal atrophy

During a median follow-up time of 668 days (Q25: 356.5, Q75: 1,231.5), 7 patients (7.7%) experienced renal atrophy, which only occurred in type 2 and type 3, with there being almost no difference (P=0.148) between the 2 types in the incidence of renal atrophy (type 3, 8.6% *vs.* type 4, 7.1%) during the similar median follow-up period: 28.2 (Q25: 12.7, Q75: 35.9) *vs.* 22.2 months (Q25: 13.4, Q75: 34.9). The Cox regression model for predicting renal atrophy is shown in *Table 3*. The univariate analysis suggested that potential predictors for renal atrophy were false lumen thrombosis in the thoracic aorta, false lumen thrombosis in the abdominal aorta and/or the renal artery, relative enhancement of the affected renal artery, extension of dissection in the renal artery, and length of TEVAR coverage. Further multivariate regression analysis identified that only false lumen thrombosis in the abdominal aorta and/or the renal artery was associated with a significantly higher risk of renal atrophy [hazard ratio (HR) =17.757; P=0.008]. In our study, 6 of the 7 (85.7%) patients with renal atrophy had partial thrombus in the abdominal aorta, and 2 of the 7 (28.6%) had dissection extending to the renal artery with thrombus in the false lumen. *Figure 4* depicts the Kaplan-Meier curves of renal atrophy according to false lumen thrombosis in the abdominal aorta and/or renal artery (log-rank, chi-square =13.626; P<0.001). *Figure 5* shows the renal artery and renal volume in a TBAD patient with renal atrophy before and after TEVAR.

Blood examination in patients with renal atrophy

Among the 7 patients with renal atrophy in our study, only 1 had both evaluated serum creatinine and urea nitrogen

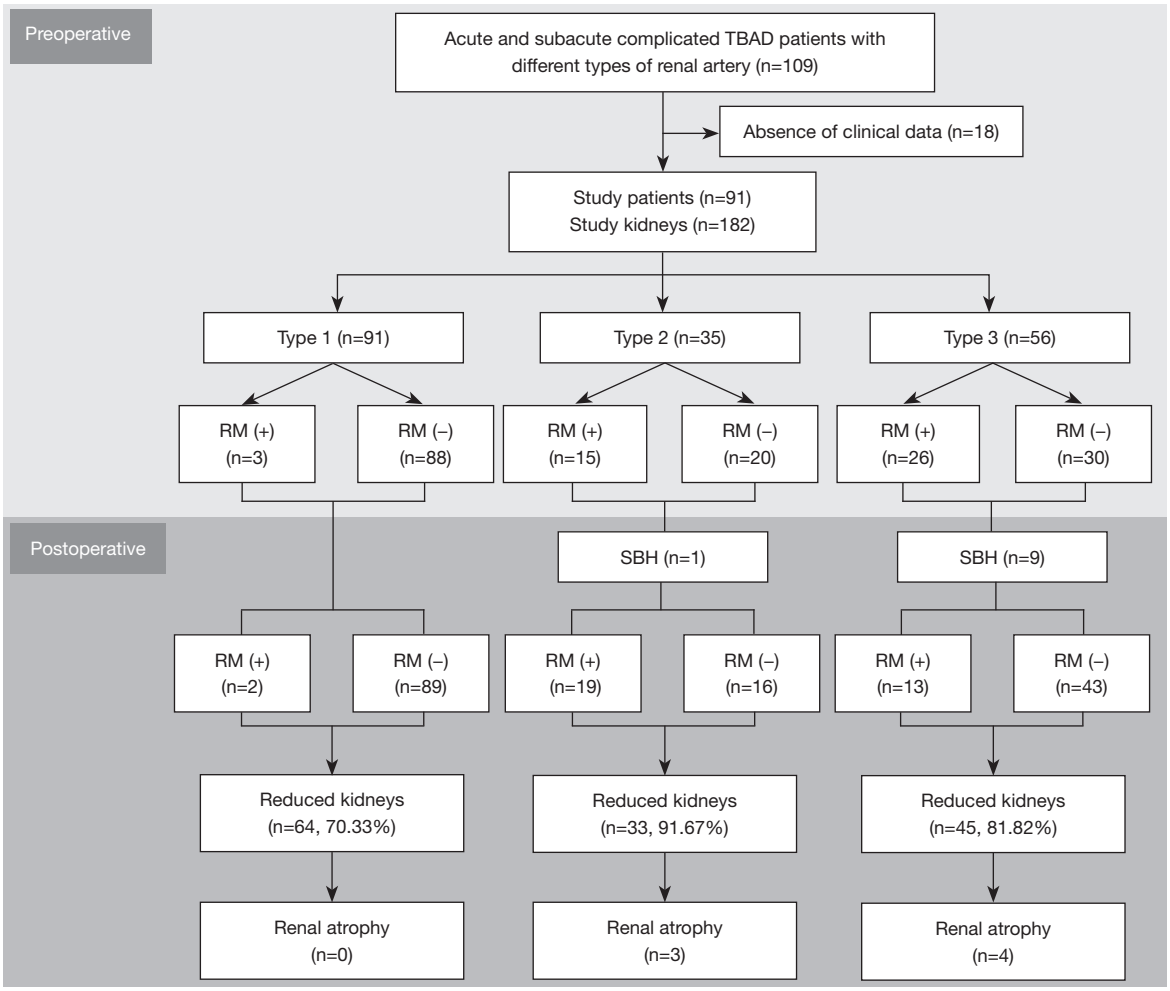

Figure 2 A branch diagram of all enrolled patients and kidneys. The branch diagram summarizes the conditions of all the renal arteries and kidneys in preoperative and postoperative aortic CTA. TBAD, type B aortic dissection; RM, renal malperfusion; SBH, spontaneous branch healing; CTA, computed tomography angiography.

Table 2 Characteristics of renal artery and kidney

Variable	Total (n=182)	Type 1 (n=91)	Type 2 (n=35)	Type 3 (n=56)	P value
Preoperative CTA					
Left renal artery:right renal artery (n:n)	–	52:39	15:20	24:32	0.152*
Renal malperfusion, n (%)	44 (24.18)	3 (3.30)	15 (42.86)	26 (46.43)	<0.001*
Renal volume (mL)	197.11±38.37	198.23±38.68	197.37±41.77	195.10±36.11	0.893 (F=0.114)
Follow-up CTA					
Spontaneous healing, n (%)	–	–	1 (2.86)	9 (16.07)	0.049*
Renal malperfusion, n (%)	–	2 (2.20)	19 (54.29)	13 (23.21)	<0.001*
Renal volume (mL)	179.29±46.88	190.09±43.25	165.15±52.63	170.70±45.28	0.006 (F=5.208)
Change of renal volume (mL)	–17.82±36.11	–8.14±29.31	–32.22±41.59	–24.41±38.44	0.001 (F=7.561)

Data are mean ± standard deviation, n (%) or (n:n). *, Pearson chi-squared test. CTA, computed tomography angiography.

before TEVAR (serum creatinine 155 μmol/L, urea nitrogen 8.87 mmol/L), and 1 had both evaluated serum creatinine and urea nitrogen in the follow-up examination (serum creatinine 227.38 μmol/L, urea nitrogen 11.68 mmol/L). The renal volume was a more sensitive indicator of renal injury than was the blood examination.

Discussion

In this study, we investigated the distribution and natural history of the involved renal artery, renal volume changes before and after TEVAR, and predictors of renal atrophy in complicated TBAD. Although TEVAR could promote the healing of a small number of renal arteries, it could not prevent kidney shrinkage. Renal atrophy only occurred in kidneys supplied by the aortic false lumen and both the aortic true and false lumen. Along with the type of renal artery, false lumen thrombosis in the abdominal aorta and/or the renal artery was found to be an independent predictor of renal atrophy.

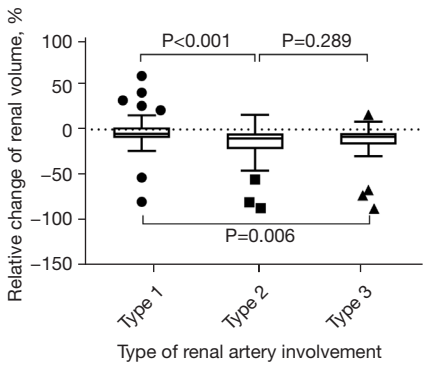

Figure 3 The turkey box figure shows the relative change in renal volume between the different types of renal artery involvement. The relative renal volume change of type 1 was significantly smaller than that of type 2 and type 3, while no significant difference was found between type 2 and type 3. The circles, squares, and triangles indicate the outliers in each type.

The renal artery was divided into 3 types according to the source of blood supply, which may affect renal perfusion (14). The affected renal artery, including types 2 and 3, was more often distributed on the right, while type 1 was more often distributed on the left. This phenomenon may occur because the dissection flap tends to lie posterolaterally and to the left of the true lumen, down to the diaphragm, and spiral downward in the abdominal aorta (15). Affected by the low-velocity blood flow from the false lumen, the incidence of renal malperfusion in the kidney supplied by types 2 and 3 renal arteries was 10 times that of the kidney supplied by the true lumen alone (type 1). However, there was no significant difference in renal volume before TEVAR, which may indicate that a temporary circulatory shock and decrease in renal blood supply has little effect on renal volume and renal function (only 5.49% with elevated blood serum creatinine and 12.09% with elevated blood urea nitrogen). After TEVAR, renal arteries originating

Table 3 Cox regression model for predicting renal atrophy

Parameters (n=91)	Renal atrophy			
	Univariate analysis		Multivariate analysis	
	HR (95% CI)	P value	HR (95% CI)	P value
FL thrombosis only in thoracic aorta	0.048 (0.006, 0.400)	0.005		
FL thrombosis in abdominal aorta and/or renal artery	17.757 (2.129, 148.073)	0.008	17.757 (2.129, 148.073)	0.008
The relative size of FL	0.293 (0.537, 5.505)	0.183		
The relative enhancement of affected renal artery	0.013 (0.001, 1.008)	0.050		
Re-entry at and above the level of renal artery	0.002 (0.001, 34.502)	0.207		
Extension of dissection in the renal artery	9.048 (1.978, 41.396)	0.005		
Length of TEVAR coverage	0.970 (0.943, 0.998)	0.039		

All parameters were assessed with CT 1 week after TEVAR. The true and false lumen size was the maximum vertical distance between the lumen wall and the tangent of the intimal flap at the level of the affected renal artery. The relative size of the false lumen was the ratio of the size of the false lumen to that of the true lumen. The relative enhancement of the affected renal artery was the ratio of the CT value of the affected renal artery to that of the true lumen at the same level. HR, hazard ratio; CI, confidence interval; FL, aortic false lumen; TEVAR, thoracic endovascular aortic repair; CT, computed tomography.

from the false lumen (type 2) rarely healed spontaneously, as the false lumen was not completely compressed. However, a small percentage (11.4%) can be converted to the cosupply of true and false lumen due to the enlargement of circumferential re-entry tear and communication of both lumens (16). Because of the expansion of the true lumen and oppression of the false lumen in the renal artery, type 3a, defined as dissection extending to the renal artery, was easier to heal. The majority (91.67%) of renal volume measures reduced in the long-term after TEVAR, regardless of the lumen from which the renal artery originated. However, renal atrophy only occurred in types 2 and 3, and there was almost no difference in the incidence between the 2 types. During follow-up, a type 1 renal artery became a double-lumen blood supply (incidence only 0.1%) due to the formation of a large re-entry tear. While the kidney was still mainly supplied with blood from the true lumen, there was little effect on renal perfusion and renal volume. The transition between different types was consistent with the previous study (1).

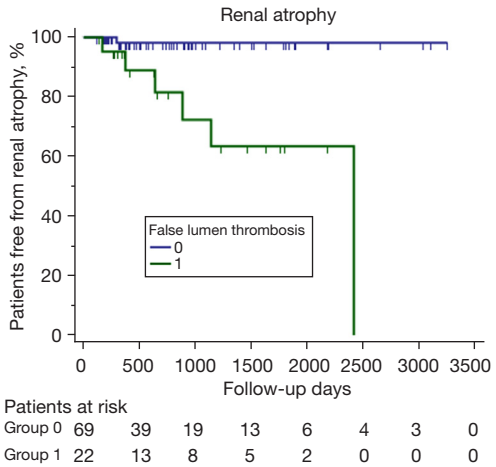

Figure 4 Kaplan-Meier curves of renal atrophy. Significantly lower event-free rates were observed in patients with thrombosis in the false lumen in the abdominal aorta and/or the renal artery (log-rank test, chi-Square =13.626; P<0.001).

In this study, the mean postoperative volume of type 1 was 190.09±43.25 mL. The renal volume was within the normal range and did not change much after TEVAR (–8.14±29.31 mL). The reduction of renal volume may be due to dynamic obstruction (7). Therefore, the evaluation of renal atrophy by bilateral renal volume ratio not only takes

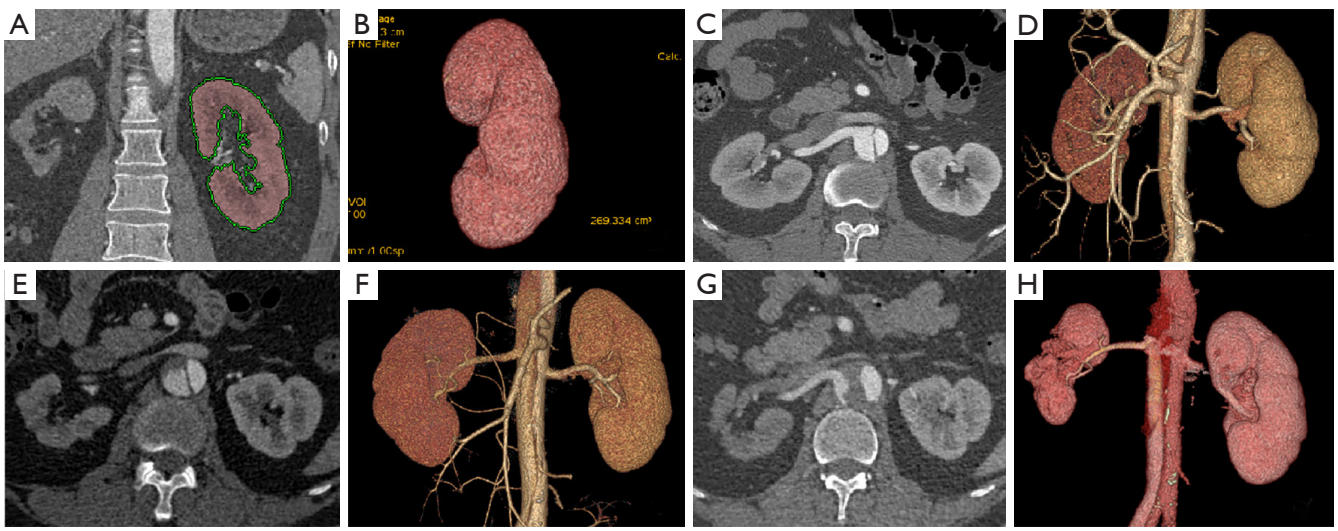

Figure 5 CT images of renal and kidney in a TBAD patient. (A,B) Show that a kidney was labeled in the postprocessing workstation, and kidney volume was semiautomatically calculated. (C-H) Show the CT images of a patient before TEVAR, 3 days after TEVAR, and 2 years and 6 months after TEVAR, respectively. (C,D) Show the preoperative CT axial and VR images. The right renal artery belonged to type 2 originating from the aortic false lumen; both kidneys were of approximately equal volume (right kidney volume: 238.42 mL; left kidney volume: 250.97 mL). (E,F) The axial CT and VR images showing partial thrombosis in the abdominal aortic false lumen; there is a small difference in volume between the 2 kidneys (right kidney volume: 200.37 mL; left kidney volume: 237.53 mL). (G,H) The axial CT and VR images showing the enlarged thrombus and right renal atrophy (right renal volume: 107.55 mL; left renal volume: 230.64 mL). CT, computed tomography; TBAD, type B aortic dissection; TEVAR, thoracic endovascular aortic repair; VR, volume rendering.

into account the reduction in renal volume due to systemic factors (such as age) but also would not miss renal atrophy evaluated by absolute value.

In addition to the type of involved renal artery, this study also found false lumen thrombosis in the abdominal aorta and/or the renal artery to independently associated with renal atrophy. The risk of renal atrophy increased 17 times in patients with thrombus compared to those without, which is consistent with the findings of a previous study (17). However, the latter study defined renal atrophy broadly, including localized and global renal atrophy, and did not locate the thrombus according to the aortic segment. Our study found no threat to renal atrophy if the thrombus existed only in the thoracic aorta. These patients did not have a thrombus in the abdominal aorta due to the re-entry tear. In another study, Wang *et al.* (8) reported renal atrophy to be predicted by the CT findings of renal artery dissection. This was not entirely consistent with our results because the enrolled patients included those with aortic dissection that stopped proximal to the level of the renal artery, and the renal volume was estimated by the ellipsoid formula of the 3-dimensional values of the kidney. We considered that dissection extending to the renal artery (type 3a) does not necessarily cause renal atrophy, which may be associated with long-term postoperative aortic remodeling and renal artery healing (1). If the true lumen is dilated and the false lumen is collapsed in the renal artery, the renal artery can completely restore the blood supply from the true lumen. In a recent study, the incidence of renal atrophy was reported to be 27.3% in patients with TBAD after TEVAR (18). The incidence was almost 3 times that found in our study (9.9%), as the enrolled patients all had decreased mean density of the unilateral renal parenchyma, which was also much higher than that in our study (24.18%). Renal atrophy was defined according to the length of the longitudinal axis of the kidney.

Study limitations

There were some limitations in our study. The inconsistency in timing of both pre- and postoperative CT examination was a limit. Since this study was a retrospective study, postoperative blood pressure could not be obtained, and its relationship with renal perfusion and renal atrophy needs further study. Moreover, study enrollment derived from a single center, which may limit the generalizability of our results to similar care settings. In addition, the gold standard of renal malperfusion is a systolic gradient of more than 15 mmHg between the aorta and the renal hilum identified by intravascular ultrasound (19). However, this was not performed, and manometric findings could not be acquired. Moreover, we did not determine the influence of renal stent placement or fenestration on renal atrophy. In the future, a large prospective study should be conducted to confirm the findings.

Conclusions

Our study examined the natural history of the involved renal artery and renal volume changes in acute and subacute complicated TBAD patients after TEVAR. Regardless of the renal artery type, TEVAR did not prevent long-term renal shrinkage. Kidneys supplied by the false lumen or both the true and false lumen shrank more significantly. Those patients with false lumen thrombosis in the abdominal aorta and/or the renal artery were more likely to experience renal atrophy. Overall, patients with type 2 or 3 renal artery and false lumen thrombosis in the abdominal aorta and/or renal artery should be monitored closely and intervened actively.

Acknowledgments

Funding: This work was supported by the Young Scientists Fund of the National Natural Science Foundation of China (No. 82000444) and the AI+ Health Collaborative Innovation Cultivation Project of Beijing Municipal Science and Technology Commission (No. Z201100005620013).

Footnote

Reporting Checklist: The authors have completed the STROBE reporting checklist. Available at https://qims.amegroups.com/article/view/10.21037/qims-21-1240/rc

Conflicts of Interest: All authors have completed the ICMJE uniform disclosure form (available at https://qims.amegroups.com/article/view/10.21037/qims-21-1240/coif). The authors have no conflicts of interest to declare.

Ethical Statement: The authors are accountable for all aspects of the work in ensuring that questions related to the accuracy or integrity of any part of the work are appropriately investigated and resolved. The study was conducted in accordance with the Declaration of Helsinki (as revised in 2013). The study was approved by the Ethics Committees of Fuwai Hospital, and informed consent was

taken from all individual participants.

References

1. Iwakoshi S, Dake MD, Irie Y, Katada Y, Sakaguchi S, Hongo N, et al. Management of Renal Arteries in Conjunction with Thoracic Endovascular Aortic Repair for Complicated Stanford Type B Aortic Dissection: The Japanese Multicenter Study (J-Predictive Study). Radiology 2020;294:455-63.
2. Gong IH, Hwang J, Choi DK, Lee SR, Hong YK, Hong JY, Park DS, Jeon HG. Relationship among total kidney volume, renal function and age. J Urol 2012;187:344-9.
3. Hueper K, Gutberlet M, Rong S, Hartung D, Mengel M, Lu X, Haller H, Wacker F, Meier M, Gueler F. Acute kidney injury: arterial spin labeling to monitor renal perfusion impairment in mice-comparison with histopathologic results and renal function. Radiology 2014;270:117-24.
4. Fann JI, Sarris GE, Mitchell RS, Shumway NE, Stinson EB, Oyer PE, Miller DC. Treatment of patients with aortic dissection presenting with peripheral vascular complications. Ann Surg 1990;212:705-13.
5. Fann JI, Smith JA, Miller DC, Mitchell RS, Moore KA, Grunkemeier G, Stinson EB, Oyer PE, Reitz BA, Shumway NE. Surgical management of aortic dissection during a 30-year period. Circulation 1995;92:II113-21.
6. Miller DC, Mitchell RS, Oyer PE, Stinson EB, Jamieson SW, Shumway NE. Independent determinants of operative mortality for patients with aortic dissections. Circulation 1984;70:I153-64.
7. Erbel R, Aboyans V, Boileau C, Bossone E, Bartolomeo RD, Eggebrecht H, et al. 2014 ESC Guidelines on the diagnosis and treatment of aortic diseases: Document covering acute and chronic aortic diseases of the thoracic and abdominal aorta of the adult. The Task Force for the Diagnosis and Treatment of Aortic Diseases of the European Society of Cardiology (ESC). Eur Heart J 2014;35:2873-926.
8. Wang CC, Lin HS, Huang YL, Wu FZ, Chuo CC, Ju YJ, Wu CC, Wu MT. Renal artery involvement in acute aortic dissection: Prevalence and impact on renal atrophy in non-interventional treatment patients. J Cardiovasc Comput Tomogr 2018;12:404-10.
9. Fang K, Zhao J, Luo M, Xue Y, Wang H, Ye L, Zhang X, Zheng L, Shu C. Quantitative analysis of renal blood flow during thoracic endovascular aortic repair in type B aortic dissection using syngo iFlow. Quant Imaging Med Surg 2021;11'3726-34.
10. D'Souza RC, Kotre CJ, Owen JP, Keir MJ, Ward MK, Wilkinson R. Computed tomography evaluation of renal parenchymal volume in patients with chronic pyelonephritis and its relationship to glomerular filtration rate. Br J Radiol 1995;68:130-3.
11. Herts BR, Sharma N, Lieber M, Freire M, Goldfarb DA, Poggio ED. Estimating glomerular filtration rate in kidney donors: a model constructed with renal volume measurements from donor CT scans. Radiology 2009;252:109-16.
12. Widjaja E, Oxtoby JW, Hale TL, Jones PW, Harden PN, McCall IW. Ultrasound measured renal length versus low dose CT volume in predicting single kidney glomerular filtration rate. Br J Radiol 2004;77:759-64.
13. Hagan PG, Nienaber CA, Isselbacher EM, Bruckman D, Karavite DJ, Russman PL, et al. The International Registry of Acute Aortic Dissection (IRAD): new insights into an old disease. JAMA 2000;283:897-903.
14. Levy D, Goyal A, Grigorova Y, Farci F, Le JK. Aortic Dissection. Treasure Island, FL, USA: StatPearls Publishing, 2022.
15. McMahon MA, Squirrell CA. Multidetector CT of Aortic Dissection: A Pictorial Review. Radiographics 2010;30:445-60.
16. Williams DM, Lee DY, Hamilton BH, Marx MV, Narasimham DL, Kazanjian SN, Prince MR, Andrews JC, Cho KJ, Deeb GM. The dissected aorta: part III. Anatomy and radiologic diagnosis of branch-vessel compromise. Radiology 1997;203:37-44.
17. Chan WH, Huang YC, Weng HH, Ko SF, Chu JJ, Lin PJ, Wan YL. Analysis of intimal extent and predictors of renal atrophy in patients with aortic dissection. Acta Radiol 2012;53:732-41.
18. Zhou M, Bai X, Cai L, Ding Y, Li X, Lin J, Fu W, Shi Z. Outcomes and Predictors of Endovascular Treatment for

Type B Aortic Dissection Complicated by Unilateral Renal Ischemia. J Vasc Interv Radiol 2019;30:973-8.
19. DiMusto PD, Williams DM, Patel HJ, Trimarchi S, Eliason JL, Upchurch GR Jr. Endovascular management of type B aortic dissections. J Vasc Surg 2010;52:26S-36S.

Cite this article as: Yu YT, Ren XS, An YQ, Yin WH, Zhang J, Wang X, Lu B. Changes in the renal artery and renal volume and predictors of renal atrophy in patients with complicated type B aortic dissection after thoracic endovascular aortic repair. Quant Imaging Med Surg 2022;12(11):5198-5208. doi:10.21037/qims-21-1240

